Journal of Crystal Growth 310 (2008) 4835–4838

Contents lists available at ScienceDirect

Journal of Crystal Growth

journal homepage: www.elsevier.com/locate/jcrysgro

Growth of various antimony-containing alloys by MOVPE

Christian Grasse [a,*], Ralf Meyer [a], Uwe Breuer [b], Gerhard Böhm [a], Markus-Christian Amann [a]

[a] *Walter Schottky Institut, Technische Universität München, Am Coulombwall 3, 85748 Garching, Germany*
[b] *Forschungszentrum Jülich, 52425 Jülich, Germany*

ARTICLE INFO

Available online 4 July 2008

Keywords:
A1. Characterization
A1. Crystal structure
A3. Metal organic vapour phase epitaxy
B1. Antimonides
B2. Semiconducting III–V materials

ABSTRACT

GaInPSb bulk and superlattice layers have been grown by metal organic vapour phase epitaxy (MOVPE) at low growth temperatures on exact and misorientated InP substrates. Optical and structural studies of the properties of the material reveal that phase separation plays an important role in the growth of this alloy, which is indicated by very broad linewidths in low-temperature photoluminescence (PL) measurements. To explain this behaviour simple miscibility gap calculations for the materials GaInPSb, GaInAsSb and GaInAsP have been performed using the regular solution model. A comparative growth analysis of GaInAsP, GaInPSb bulk and InPSb, GaInAsSb and GaAsSb superlattice structures showed that just the phosphorus- and antimony-containing alloys exhibited the broad low temperature (4 K) PL linewidths (FWHM) of about 50–100 meV. So it can be assumed that due to the large difference in binding energies phosphorus-containing antimonides require much more effort for good crystal quality than equal arsenical alloys.

1. Introduction

Antimonides have become more and more interesting in the past few years due to their use for solar or thermophotovoltaic applications and as infrared light-emitting lasers [1]. Besides the low bandgap, antimonides feature a type-II band alignment, which is utilized for "W"-shaped quantum wells [2], but offer also an important improvement for electrical tunable lasers based on the plasma effect [3]. Such InP-based devices are essential components for various telecommunication applications and have received considerable attention in recent years [4]. Previous results of fabricated tunable lasers like the sampled grating tunable twin guide laser (SG-TTG) showed the state of the art performance with a tuning range of over 40 nm, a single-mode output power of 10 mW and high side-mode suppression [5], but will suffer from high tuning currents due to the recombination of charge carriers in the direct semiconductor of the tuning region. To overcome this drawback an indirect semiconductor would be the ideal choice. Furthermore, the material system should be aluminum-free, since the fabrication of such a laser device requires several selective overgrowth steps. Unfortunately there is no such material that can be grown lattice-matched to InP. Therefore the best approximation would be a type-II superlattice where direct recombination is suppressed via the band structure. This kind of bandgap engineering can be achieved when antimony is incorporated into the crystal.

Antimony-containing alloys like GaAsSb and GaInAsSb have been already investigated for the realization of a type-II heterostructure on InP substrate, but due to the low bandgap of these ternary and quaternary compounds the benefit of the enhancement of the type-II band alignment would be lost by fundamental absorption in the case of lasers emitting at 1.55 μm, the main telecommunication wavelength.

The barely explored material system GaInPSb in combination with GaInAsP besides provides a type-II band alignment also provides a considerably higher bandgap for such lasers and would therefore be the material combination of choice and was investigated in this work.

Since previous growth studies of GaInPSb have been just done by Jou et al. [6] with an atmospheric pressure metal organic vapour phase epitaxy (AP-MOVPE) and by Köhler et al. [7] with a gas source MBE, the first results of this alloy grown by low-pressure MOVPE (LP-MOVPE) will be presented in this paper. In addition to give a comparison of the crystal quality and the applicability for devices between phosphorus- and arsenic-containing antimonides also the growth of InPSb, GaAsSb and GaInAsSb has been investigated mainly by photoluminescence (PL) measurements and will be discussed.

2. Experimental procedure

All (GaIn)(PSb) and (GaIn)(AsSb) layers were grown in a commercially available horizontal reactor system (AIX 200/4) by MOVPE using purified H_2 carrier gas at a reduced reactor pressure

---

[*] Corresponding author. Tel.: +49 89 289 12789; fax: +49 89 320 6620.
E-mail address: grasse@wsi.tum.de (C. Grasse).

0022-0248/$ - see front matter © 2008 Elsevier B.V. All rights reserved.
doi:10.1016/j.jcrysgro.2008.06.078

of 150 mbar and a total gas flow of 10 l/min. As a result of the metastability of antimony-containing alloys low substrate temperatures in the range of 500–575 °C have been chosen. For group III deposition trimethylgallium (TMGa), TMIn, triethylgallium (TEGa) and on the group V side phosphine, arsine and TMSb were deployed on exactly orientated, as well as 2° and 6° misorientated InP and for the growth of GaAsSb exactly orientated GaAs substrates. Besides GaInPSb and GaInAsP bulk layers, also GaInAs/GaInAsSb, InP/InPSb and GaAs/GaAsSb superlattice structures with well and barrier widths of 4 and 20 nm, respectively, have been grown. In each case a 10-s growth interruption under arsine or phosphine gas flow prior to and after the antimony-containing well has been performed. Before starting the growth all layers have been heated up to 660 °C under phosphine and arsine stabilisation, for oxide desorption, and also to achieve reproducible growth conditions.

The layers have been characterised with X-ray diffraction (XRD) using a Stoe single monochromator diffractometer, van der Pauw Hall measurements, TOF-SIMS and XPS measurements, which were carried out at the Forschungszentrum Jülich. For low- and room-temperature PL measurements a frequency doubled Nd:Yag laser emitting at 532 nm has been used for excitation.

3. Results and discussion

In this section, first the approach to analyse the growth behaviour of $Ga_xIn_{1-x}P_ySb_{1-y}$ on InP substrate is introduced and the results are compared with the well-explored $Ga_xIn_{1-x}As_yP_{1-y}$ material system. Then the optical properties obtained by PL measurements of both alloys are discussed. Based on miscibility gap calculations, which are shortly explained, these optical characterisations are also conferred with the measurements of InPSb, GaASb and GaInAsSb layers.

To achieve a comprehensive understanding of the growth of GaInPSb on InP substrate, all possible lattice-matched compositions starting from InP and going to $GaP_{0.35}Sb_{0.65}$ by gradual increase of TMGa and TMSb mass flow have been tried to be synthesized. First mirror-like layers were grown with TMGa, TMIn, PH_3 and TMSb at a substrate temperature of 575 °C, which is the highest usually used growth temperature for GaInAsSb and not too far away from the optimal temperature of 650 °C for GaInAsP layers. By attempting to reach gallium- and antimony-rich compositions an increasing group V incorporation coefficient C_V was recognized by XRD and PL measurements, assuming a constant group III incorporation coefficient C_{III} taken from a lattice-matched GaInAs layer grown at 575 °C. From the definition of these coefficients,

$$\frac{Q_{PH_3}}{Q_{TMSb}} C_V = \frac{y_P}{1-y_P}$$

$$\frac{Q_{TMGa}}{Q_{TMIn}} C_{III} = \frac{x_{Ga}}{1-x_{Ga}}$$

where Q is the gas flux in μmol/min. It is easy to see that increasing C_V coefficient means a saturation of the antimony content in the solid. Although more TMSb is provided in the vapour phase the phosphorus gets better incorporated into the crystal. A comparison with the incorporation behaviour of GaInAsP in Fig. 1(a) shows that here the incorporation index, as determined from PL and XRD measurements, stays constant; thus the growth process of GaInPSb is quite unusual. Additionally a morphological degradation was observed, when the PH_3/TMSb ratio was reduced even further. To measure the direct elemental composition and to verify these results, SIMS measurements of several GaInPSb layers grown at 550 °C with increasing TMGa and TMSb concentration in the gas phase have been carried out. As can be seen in Fig. 1(b) both the group III and the group V incorporation indexes are not remaining constant, resulting in a saturation of x_{Ga} at 30% and of y_{Sb} at 15% (Table 1). This tendency was also confirmed by XPS measurements.

Due to the saturation of the gallium composition, growth rate and growth efficiency *f*, which means growth rate divided by the pseudomorphic lattice constant and the respective group III mass flow, are found to decrease by increasing TMGa/TMIn ratio in the vapour. This trend resulted in the observation that no growth of GaPSb with phosphine, TMSb and TMGa could be observed by XRD and so were angular cut measurements. Based on the fact that the growth of GaInSb, GaInP and InPSb could be verified by using TMGa, TMIn, TMSb and phosphine, and additionally also GaPSb could be grown by exchanging TMGa with TEGa, a parasitic vapour reaction between TMGa, TMSb and phosphine is supposed, which would explain the shrinkage of the TMGa growth efficiency in Table 1.

To summarize the results of the growth analysis of GaInPSb it can be noted that a saturation of the group III and group V composition was also found by Jou et al. for atmospheric

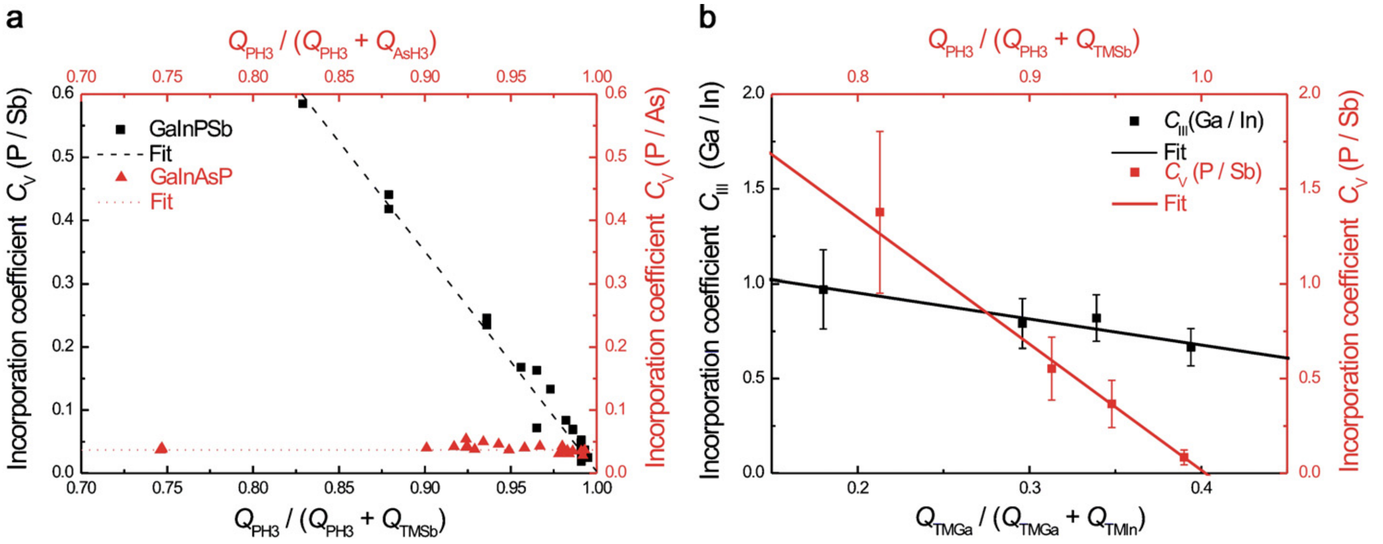

Fig. 1. The group V incorporation index of GaInPSb against the vapour supply is faced with GaInAsP (a) and (b) shows the incorporation indexes measured by SIMS of GaInPSb layers grown at 550 °C.

Table 1
SIMS and PL measurements (at 4 K) of 1-μm thick GaInPSb bulk layers grown at 550 °C

Sample ID	Q_{TMGa}/Q_{TMIn}	Q_{PH3}/Q_{TMSb}	x_{Ga}	y_P	f_{TMGa} (1/μmol s)	f_{TMIn} (1/μmol s)	PL E_{Peak} (eV)	PL FWHM (meV)
V0241	0.22	103	0.18	0.90	0.0212	0.0219	1.016	107
V0240	0.42	18	0.25	0.87	0.0201	0.0254	0.939	61
V0350	0.51	10	0.30	0.85	–	–	0.909	80
V0244	0.65	4	0.30	0.86	0.0170	0.0256	0.909	75

The growth rate was determined by surface profile measurements.

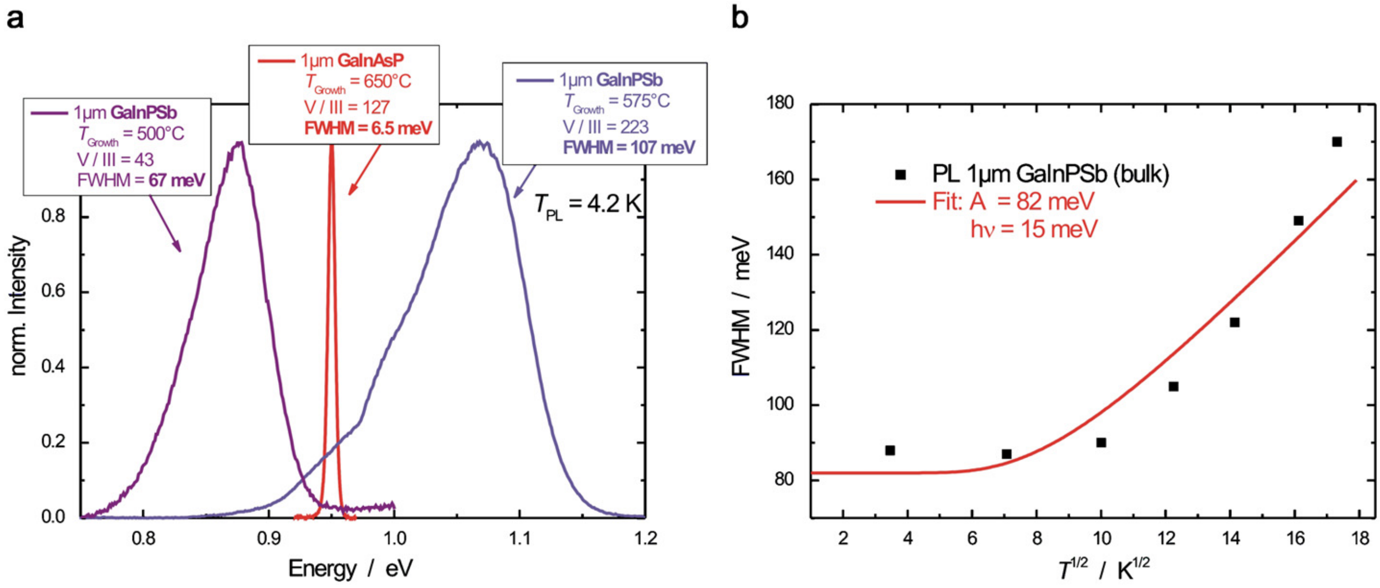

Fig. 2. (a) 4 K PL measurements of GaInPSb and GaInAsP bulk layers and (b) illustration of the temperature dependence of the GaInPSb layer PL linewidth. The red fit is calculated with the cc-model.

MOVPE [7]. Surprisingly the growth of GaPSb with TMGa, TMSb and phosphine was also reported [8], which could not be achieved in this study.

Besides the incorporation behaviour, also the crystal quality was investigated by PL measurements. Fig. 2(a) shows the normalized 4 K PL spectra of two GaInPSb layers with very different growth parameters compared to a GaInAsP PL measurement. Obviously the linewidths (FWHM) of the GaInPSb spectra were more than 10 times higher than that of GaInAsP, which indicates a very poor layer quality. Aware of the fact that the broadening due to alloy scattering would be expected to be close to 10 meV considering the formula of Schubert et al. [9], other reasons like high background doping, contaminated precursors and clustering effects have been reviewed. However, Hall measurements indicated a low n-doping concentration of 10^{15}–$10^{16}\,cm^{-3}$ with expectable mobilities of about 2000–3000 $cm^2/V\,s$. Also an exchange of the TMSb precursor revealed no improvement, so a contaminated precursor could be excluded as a reason for this broadening.

Finally, clustering phenomena have been taken into account as an explanation for this broadening, which is a well-known issue in the growth of antimonides [10]. It appears also to be the only explanation for the further broadening of the GaInPSb PL linewidth illustrated in Fig. 2(b), when the temperature is increased. Since usually the temperature-dependent broadening would be caused by the thermal broadening of the reachable density of states, which is $1.8\,k_BT$ for Maxwell–Boltzmann statistics [9] and therefore about 50 meV at room temperature, a phonon-activated defect complex based on the configuration coordinate model of Klick and Schulman [11] would explain the observed temperature behaviour of the PL linewidth:

$$\mathrm{FWHM}(T) = A\left[\coth\left(\frac{h\nu}{2k_BT}\right)\right]^{1/2}$$

where A is the half width at temperatures near to 0 K and $h\nu$ the energy of the vibrational mode of the excited state of the defect centre [12]. This complex is supposed to be induced by phase separation effects and would reduce the applicability for devices.

To encourage these findings, miscibility gap calculations for GaInAsP, GaInAsSb and GaInPSb have been performed using the regular solution model [13] with parameters taken from Ref. [14]. From these calculations a temperature T_C, the so-called critical temperature, was obtained. This temperature has to be reached for the growth of high-quality randomized alloys [15]. The higher the critical temperatures, the stronger are the differences in the bonding strength of the various atoms and hence the stronger is the tendency for clustering. As shown in Fig. 3 GaInPSb exhibits the largest miscibility gap; so phase separation is likely to occur, and also the solubility of antimony is expected to be very low [16], which would explain the antimony saturation effect discussed above. At last, Fig. 4 shows a comparison of arsenic- and phosphorus-containing antimonides, which reveals together with Fig. 1(a) the supposed coherences. The broad spectra of GaInPSb and InPSb with FWHM in the range of 50–100 meV, which have been also reported by Jaw et al. [17] and Reihlen et al. [18], and the comparatively sharp spectra of GaInAsSb and GaAsSb accord the trend from the miscibility calculations.

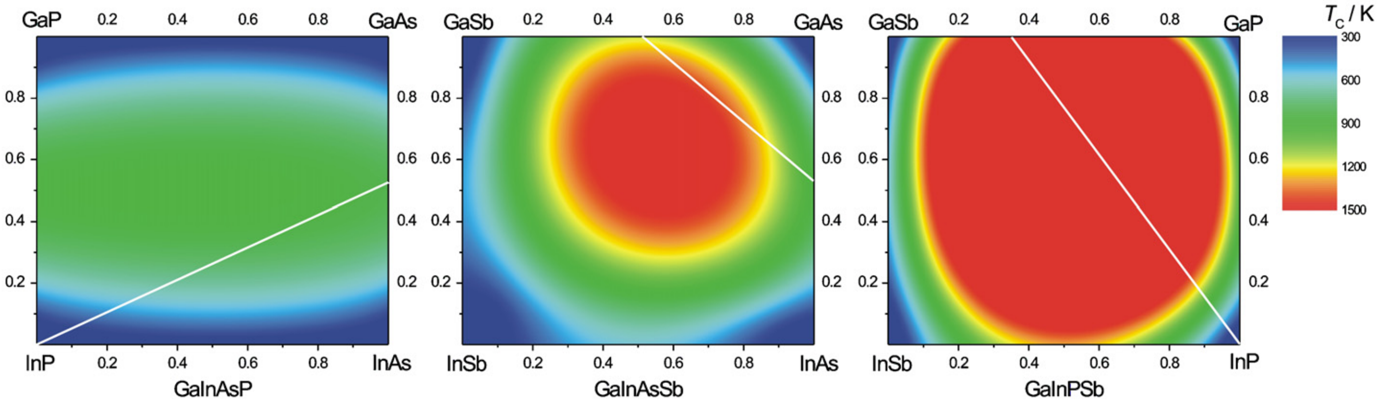

Fig. 3. Calculation of the critical temperature for GaInAsP, GaInAsSb and GaInPSb after Refs. [13,14]. The white line indicates the lattice-matching condition to InP substrate.

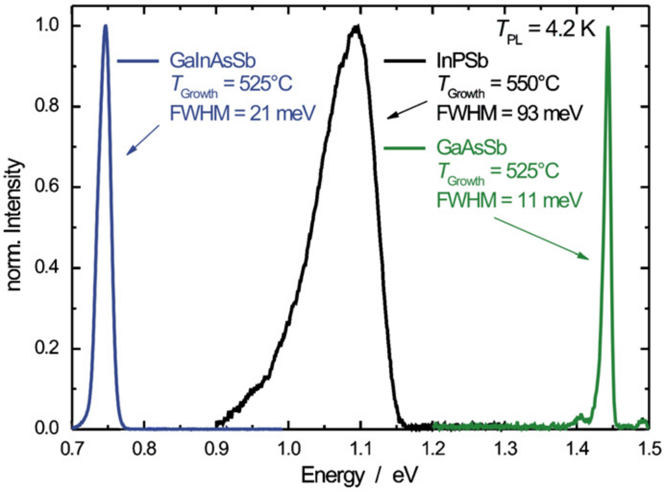

Fig. 4. Comparison of low temperature (4 K) PL spectra of InPSb, GaAsSb and GaInAsSb superlattices.

To avoid clustering, the migration length of the adsorbed atoms at the growth surface has to be reduced [19]. Hence, no ordering phenomena appear and the atoms are randomly built into the crystal. Therefore, besides the growth temperature, which could not be further decreased below 500 °C regarding the decomposition of the source molecules, substrates with miscut angles have been varied from exact to 2° and 6°, which has a large effect in the case of GaInAsSb growth [10]. However, no significant effect could be measured.

Since Szczesk et al. [20] already observed phase separation in a $Ga_{0.84}In_{0.16}As_{0.12}Sb_{0.88}$ layer direct by TEM measurements, it is evident that in the case of GaInPSb growth temperatures below 500 °C are needed to prevent clustering.

4. Conclusions

Growth and PL studies of the GaInPSb alloy at various temperatures have been presented. An unexpected growth behaviour resulting in a saturation of the gallium and antimony composition in the solid was observed, which could be explained on group III side by a parasitic vapour reaction and on group V side by the large enthalpy of mixing and therefore a strong segregation of antimony to the surface. Optical properties revealed broad linewidths and hence a poor crystal quality, which was supposed to be affected by phase separation. Although no direct investigation of clustering by TEM has been carried out, obvious reasons like background doping and precursor quality have been excluded. Therefore there are many evidences for the claim that phosphorus-containing antimonides demand extraordinary growth parameters like extremely low substrate temperatures for achieving a good crystal quality.

References

[1] F. Dimroth, C. Agert, A.W. Bett, J. Crystal Growth 248 (2003) 265.
[2] J.Y.-T. Huang, D.P. Xu, L.J. Mawst, T.F. Kuech, I. Vurgaftman, J.R. Meyer, IEEE J. Sel. Top. Quantum Electron. 13 (7) (2007) 1065.
[3] G. Rösel, F. Köhler, R. Meyer, M.-C. Amann, Semicond. Sci. Technol. 18 (2003) 325.
[4] L.A. Coldren, IEEE J. Sel. Top. Quantum Electron. 6 (6) (2000) 988.
[5] R. Todt, T. Jacke, R. Meyer, R. Laroy, G. Morthier, M.-C. Amann, IEEE J. Sel. Top. Quantum Electron. 13 (5) (2007) 1095.
[6] M.J. Jou, D.H. Jaw, Z.M. Fang, G.B. Stringfellow, J. Crystal Growth 106 (1990) 208.
[7] F. Köhler, G. Böhm, R. Meyer, M.-C. Amann., Appl. Phys. Lett. 87 (3) (2005) 032102.
[8] M. Jou, Y.T. Cherng, H.R. Jen, G.B. Stringfellow, Appl. Phys. Lett. 52 (7) (1988) 549.
[9] E.F. Schubert, E.O. Göbel, Y. Horikoshi, K. Ploog, H.J. Queisser, Phys. Rev. B 39 (2) (1984) 813.
[10] C.A. Wang, J. Crystal Growth 272 (2004) 664.
[11] C.C. Klick, J.H. Schulman, Solid State Phys. 5 (1957) 100.
[12] E.W. Williams, Phys. Rev. 168 (3) (1968) 922.
[13] V.S. Sorokin, S.V. Sorokin, A.N. Semenov, B. Ya Meltser, S.V. Ivanov, J. Crystal Growth 216 (2000) 97.
[14] K. Nakajima, Jpn. J. Appl. Phys. 38 (1999) 1875.
[15] G.B. Stringfellow, J. Electron Mater. 11 (5) (1982) 903.
[16] I. Ho, G.B. Stringfellow, J. Crystal Growth 178 (1997) 1.
[17] D.H. Jaw, M.J. Jou, Z.M. Fang, G.B. Stringfellow, J. Appl. Phys. 68 (7) (1990) 3538.
[18] E.H. Reihlen, M.J. Jou, Z.M. Fang, G.B. Stringfellow, J. Appl. Phys. 68 (9) (1990) 4604.
[19] G.B. Stringfellow, J. Crystal Growth 65 (1983) 454.
[20] P. Szczeszk, A. Amariei, J. Schöne, G. Zoulis, N. Vouroutzis, E.K. Polychroniadis, D. Stroz, J. Microscopy 224 (2006) 121.